

Studies of Electroless Copper Plating on Poplar Veneer

Tongcheng Guo, Yu Wang, and Jintian Huang *

Copper coating was deposited on poplar veneer using different relative concentrations of plating solution. The coating structure, thickness, crystal structure, surface resistivity, contact angle, surface free energy, and electromagnetic shielding effectiveness were investigated. The surface morphology and thickness were observed using scanning electron microscopy, and the crystal structure was analyzed using X-ray diffraction. Increasing the relative concentration of plating solution resulted in a uniform and dense coating structure, and the thickness notably increased. In addition, the lateral direction resistivity was two times greater than the longitudinal direction resistivity, and the surface wettability changed from hydrophilic to hydrophobic, which led to a decline in surface free energy. Electromagnetic shielding effectiveness reached 62 dB in the frequency range of 10 kHz to 1.5 GHz. The electroless plating copper veneer was optimal when the solution contained 80 g/L of $\text{CuSO}_4 \cdot 5\text{H}_2\text{O}$, 20 g/L of $\text{C}_4\text{O}_6\text{H}_4\text{KNa}$, 40 g/L of EDTA-2Na, and 40 mL/L of HCHO 40 mL/L.

Keywords: Plating copper; Relative concentration; Contact angle; Surface free energy; Electromagnetic shielding effectiveness

Contact information: College of Material Science and Art Design, Inner Mongolia Agricultural University, Hohhot 010018, China; *Corresponding author: jintian_h@163.com

INTRODUCTION

Although there are many benefits and conveniences from using electronic products, electromagnetic radiation pollution does damage to the environment and human health (Hanada *et al.* 2002). The application of electromagnetic shielding material is the most effective way to solve this problem. Electromagnetic shielding materials come in various forms and types. A wood-metal composite material is ideal because wood is a renewable resource (Sittisart *et al.* 2014). Wood exhibits unique mechanical properties, including visual, temperature, and humidity regulation (Liu 2003; Wang *et al.* 2011). Wood-metal composite material successfully combines these two discrepant materials, while retaining the benefit of wood qualities. Composite material contains both low weight and high intensity just like wood; moreover, composite also has excellent electrical and thermal conductivity which is contributed by its metal component.

The preparation of wood-metal composite material requires the inclusion of electronic conductive materials, such as metal powder, metal fiber, metal mesh, metal foil (Zhu *et al.* 2001; Zhang and Liu 2005; Pi *et al.* 2006), magnetron reactive sputtering coating (Oka *et al.* 2002, 2004), and electroless plating (Huang and Zhao 2004; Wang *et al.* 2004a,b; Huang and Zhao 2006). Electroless plating is one of the most effective methods for the following reasons: the preparation process is simple; it imparts excellent electrical

conductivity and electromagnetic shielding performance; it is lightweight; the physical and chemical properties of wood are unaltered; and it is relatively inexpensive.

Previous research of electroless-plated copper has focused on the selection of coating elements, the electrical conductivity, and the electromagnetic shielding effectiveness (Wang *et al.* 2006, 2013). However, there has been limited research on the effects of the relative concentration of plating solution on the structure and thickness of the coating and the relationship between the contact angle and the surface free energy. Therefore, a structural analysis of the coating and thickness was conducted to determine the effect of different solution concentration on coating. This study evaluated the relationships between the coating structure, thickness, surface resistivity, contact angle, and surface free energy. Additionally, the electromagnetic shielding effectiveness was used to determine the optimal solution formulation.

EXPERIMENTAL

Materials

Poplar veneer was obtained from the Sen Ming wood product factory, Hebei Province, China, with a thickness of 1 mm and format for $\phi 11.5$ mm. The electroless plating solution included the chemical reagents in Table 1 mixed with deionized water.

Table 1. Conditions for Electroless Deposition

Component	Contents
CuSO ₄ ·5H ₂ O	40 g/L
C ₄ O ₆ H ₄ KNa	10 g/L
EDTA-2Na	20 g/L
HCHO	20 mL/L
pH	11.5
Temperature (°C)	60

Preparation of Wood Metallization

Veneer pretreatment

First, the veneer surface was sanded with #600 sand paper and submerged in 90 °C distilled water for 30 min. The veneer was soaked in CuSO₄ solution for 10 min and then transferred to NaBH₄ solution for 90 s (the activation step).

Electroless copper plated veneer

The concentration of the stock plating solution was 1.0 when it was prepared according to the formulation in Table 1. The dilution ratios were 0.5, 1.0, 1.5, and 2.0 (Table 2). The solutions were heated to 60 °C, and 10% NaOH solution was added to adjust the pH to 11.5. Next, HCHO was added to the solution under continuous stirring. The veneer (in solution form) was constantly stirred for 40 min, while the pH was maintained within a stable range using NaOH. After the reactions ran to completion, the veneer was dried for 30 min in a vacuum oven (DH-101-2-S-type, YI HENG Scientific Instruments, Shanghai China) to measure the material properties.

Table 2. Relative Concentrations of Plating Solution

Series	Concentrations of Plating Solution
0.5	CuSO ₄ ·5H ₂ O 20 g/L; C ₄ O ₆ H ₄ KNa 5 g/L; EDTA-2Na 10 g/L; HCHO 10 mL/L
1.0	CuSO ₄ ·5H ₂ O 40 g/L; C ₄ O ₆ H ₄ KNa 10 g/L; EDTA-2Na 20 g/L; HCHO 20 mL/L
1.5	CuSO ₄ ·5H ₂ O 60 g/L; C ₄ O ₆ H ₄ KNa 15 g/L; EDTA-2Na 30 g/L; HCHO 30 mL/L
2.0	CuSO ₄ ·5H ₂ O 80 g/L; C ₄ O ₆ H ₄ KNa 20 g/L; EDTA-2Na 40 g/L; HCHO 40 mL/L

Characterization

Scanning electron microscopy (SEM)

The coating surface morphology and cross section were obtained using a Quanta scanning electron microscope (FEG-QUANTA650, FEI Co., Hillsboro, OR, USA).

X-ray diffraction (XRD)

X-ray diffraction was conducted on an XRD-6000 diffractometer (Shimadzu, Tokyo, Japan) to characterize the crystal structure of the copper (Cu) veneer and determine the grain size (Cu target, $\lambda = 0.154056$ nm, scanning range 20° to 80°, and scanning speed of 2°/min). Jade 5.0 software (Materials Data Inc., Livermore, CA, USA) was used to analyse XRD patterns in the diffraction angle ranged from 20° to 80°.

Electrical property

The resistance and conductivity of the plated wood surface was tested via a FT-201 four-point probe resistance meter (Four Probes Technology Company, Guangzhou, China) in the longitudinal and lateral coating directions. Four replicates from every sample was tested in order to calculate the average value.

Wettability and surface free energy

The wettability of the coating was observing via a JYSP-180 meter (JinSheng Xin Company, Beijing, China), which tests for different surface contact angles of the copper veneer (Table 3). According to Fowkes's equations (Li *et al.* 2015), the surface free energy was calculated as follows:

$$\gamma_i = \gamma_i^p + \gamma_i^d \quad (1)$$

$$\gamma_L(1 + \cos \theta) = 2\sqrt{\gamma_s^d \gamma_L^d} + 2\sqrt{\gamma_s^p \gamma_L^p} \quad (2)$$

Table 3. Surface Tension Components of the Liquid

	γ_L (mJ/m ²)	γ_L^d (mJ/m ²)	γ_L^p (mJ/m ²)
Water	72.8	21.8	51.00
Diiodomethane	50.80	50.80	0

Electromagnetic shielding effectiveness

In accordance with the method of Chinese industrial standard SJ20524-95 (SJ20524), vertical flange coaxial test equipment (DN15115, Southeast University, Nanjing, China), was used to test the electromagnetic shielding effectiveness and the test frequency range from 0.3 MHz to 1.5 GHz.

RESULTS AND DISCUSSION

Morphology

Figure 1 shows the effects of different relative concentration solutions on the veneer surface morphology. All of the veneer surfaces were covered with a metallic copper film. The entire coating layer was distributed by independent micron mastoid structures. The microscopic imaging clearly shows that each micron mastoid structure was complemented by different layers of sub-micron scale bump structures. In addition, these layered bump structures were incorporated into the bottom surface of the copper coating. Thus, the coating surface exhibited a typical secondary hierarchy classification. After the formation of the basic structure layer of submicron coating, it was gradually superimposed on the micron mastoid structure until a complete veneer coating was formed.

Figures 1a and 1b demonstrate that at a low relative concentration (0.5 and 1.0), approximately 20 μm wide fractures developed in the coating layer. In addition, small vacancy defects were noted, which commonly result in areas of low flatness and poor density. When the relative concentration was high (1.5 and 2.0), there was no apparent fracturing (Figs. 1c, d). These results indicate that the natural defects of wood were completely covered by the copper coating, and only voids generated defects during copper plating. Consequently, as the relative concentration increased, the number of areas affected declined, and the coating appeared more smooth and compact.

In Fig. 1d, the coating appeared mostly uniform and compact, and there were minimal vacancies. The entire coating layer exhibited good continuity. In the enlarged image, the micron mastoid structure was uniform in size and condensed in structure. The surface morphology at the relative concentration of 2.0 was optimal.

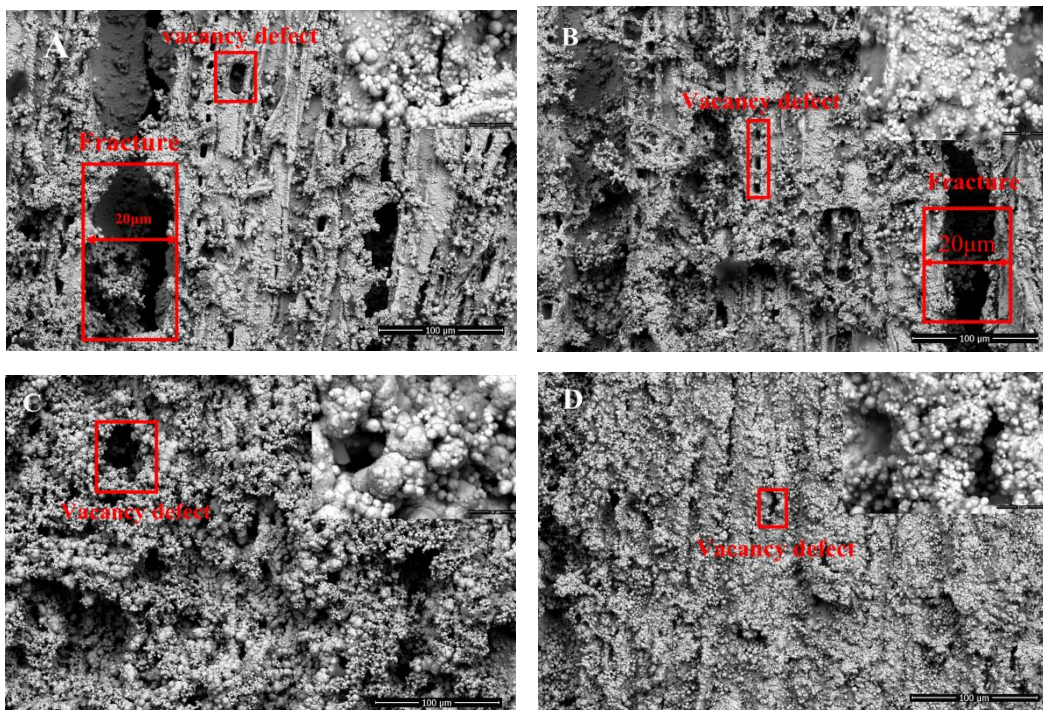


Fig. 1. Surface morphology of metallized poplar veneer at different relative concentrations: A) 0.5; B) 1.0; C) 1.5; D) 2.0. Inset images show the amplification (10000 \times)

Cross-Sectional Morphology

Figure 2 shows the copper coating thickness of a veneer cross-section. The copper coating thickness increased gradually from 62.86 μm to 132.5 μm , which was two times the original thickness (Table 4). Figure 2a shows that the copper grains were piled relatively loosely, and some clear cracks appeared. This cracking could have been attributed to the relatively low concentration (0.5 and 1.0), which slowed the reaction rate and reduced the total amount of restored metal, leading to incomplete coverage of natural wood surface defects. Therefore, the copper coating exhibited poor quality. Figures 2b and c show that the metal coating thickness increased along with the relative concentration and showed a trend for the copper grains to become more compact and uniform. Figure 2d shows that the copper grains formed a very dense coating, with a copper coating thickness of 132.5 μm ; therefore, the coating characteristics were optimal.

The inset of Fig. 2d shows the sample cross-sectional view of the relative concentration 2.0. There were two layers present: the veneer and the copper coating. The coating layer completely covered the surface of the veneer, and the veneer and the metal coating interacted through a mechanical coupling link.

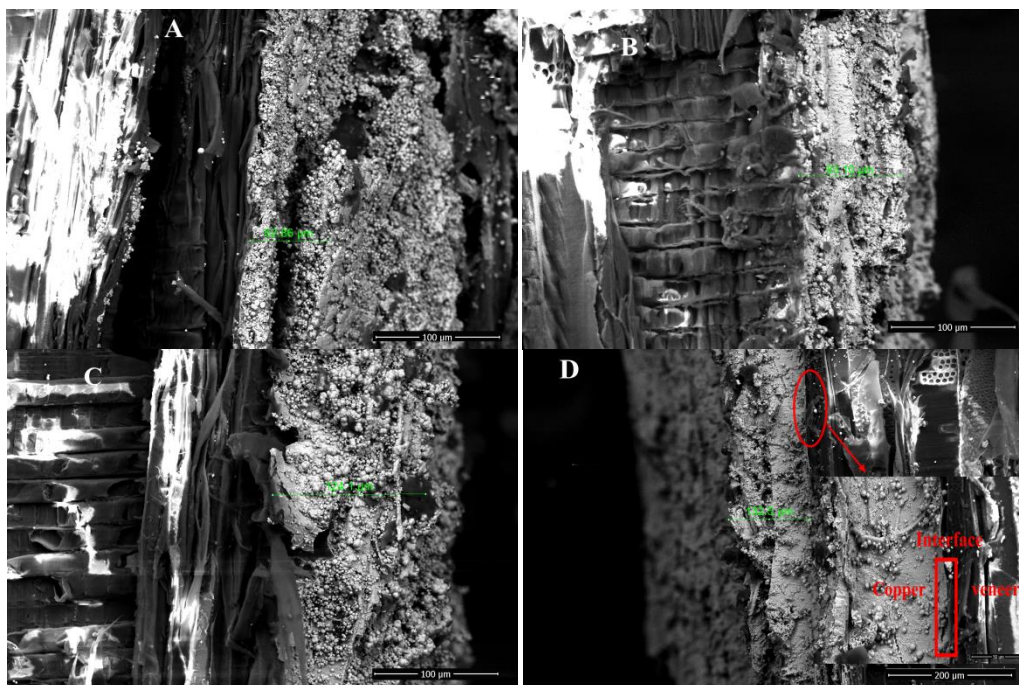


Fig. 2. Cross-sectional morphology: A) 0.5; B) 1.0; C) 1.5; and D) 2.0. The thickness was 62.66 μm , 83.1 μm , 124.1 μm , and 132.5 μm , respectively. The inset shows the coating and veneer interface (2000 \times).

Table 4. Coating Thickness of Different Relative Concentrations

Relative concentration	Thickness (μm)
0.5	62.66
1.0	83.10
1.5	124.10
2.0	132.5

X-Ray Diffraction Analysis

Figure 3a shows the poplar veneer XRD pattern. At $2\theta = 22^\circ$, it appeared that the diffraction peaks were characteristic of cellulose, although obvious features were amorphous. However, in Fig. 3b, the XRD patterns reflected crystalline structures, and the diffraction peaks of Cu (111), Cu (200), and Cu (220) occurred. Therefore, these diffraction peaks indicated the presence of copper on the poplar veneer surface. A comparison of Figs. 3a and 3b showed that the surface structure of the veneer shifted from amorphous to crystalline. The $2\theta = 22^\circ$ of the cellulose diffraction peaks disappeared, thereby showing that the veneer surface was nearly completely covered in copper.

The diffraction peaks from Fig. 3b at $2\theta = 44.12^\circ$, 51.21° , and 75.40° were compared with the reference PDF card 04-0836 (Copper standard pattern), and face-centered cubic copper diffraction peaks were identified. In addition, as the concentration increased, the half-peak width decreased, and the diffraction peaks became more pointed. According to Table 4, the copper grain size on the veneer surface was enlarged by increasing the relative concentration of the plating solution.

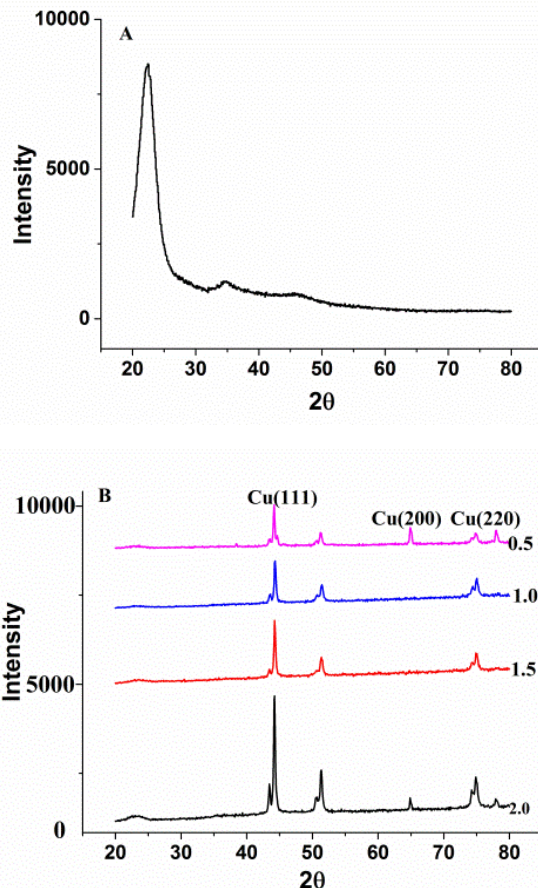


Fig. 3. X-ray diffraction analysis of A) uncoated poplar veneer and B) coated poplar veneer at the relative concentrations of 0.5, 1.0, 1.5, and 2.0

A comparison of Fig. 3b at $2\theta = 42.40^\circ$, 50.85° , 65.59° , and 73.69° and the reference PDF card 65-3288 (copper oxide standard pattern) allowed the identification of the coating layer from the crystal structure of Cu_2O . During the veneer plating processing,

elemental copper is oxidized to produce microcrystalline Cu₂O. Using the Scherrer formula (Eq. 3), the half-peak width measured from Cu (111) crystal plane was used to calculate the copper grain size,

$$D = \frac{k\lambda}{\beta \cos \theta} \quad (\text{Scherrer formula}) \quad (3)$$

where k is the Scherrer constant (1), D is the average grain thickness (nm) in the perpendicular direction of the crystal plane, β is the half-width of the diffraction peak, and λ is the X-ray wavelength. Table 5 clearly shows that the copper plating grain size increased from 17.4 nm to 30.7 nm as the solution relative concentration increased.

Table 5. Integral Breadth and Calculated Crystallite Size

Relative Concentration	Integral Breadth (β ; radians)	Crystallite Size (nm)
0.5	0.504	17.4
1.0	0.403	22.0
1.5	0.335	26.8
2.0	0.347	30.7

Surface Resistivity

Figure 4 demonstrates that as the relative concentration increased, the poplar veneer surface resistivity in the longitudinal and lateral directions tended to decrease, and the conductivity increased. This effect was especially apparent for the coating thickness because when it increased from 83.1 μm to 132.5 μm , the resistivity in both directions decreased rapidly. Thus, the coating layer shifted towards greater uniformity and condensable conditions. In addition, as the copper grain size gradually increased, forming a conductive circuit, the copper coating layer was reduced, improving the conductivity. The results from this experiment also indicated that the surface resistivity of copper-coated poplar veneer exhibited profound differences in the longitudinal and lateral directions. The resistivity of the lateral direction was twice that of the longitudinal direction; the surface resistivity showed anisotropy.

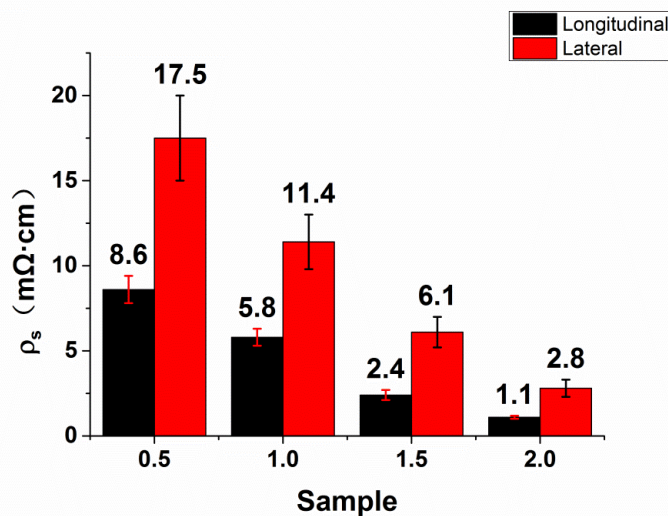


Fig. 4. Resistivity of electroless copper plated veneer in the lateral and longitudinal directions

There are two possible reasons for these differences. First, the low concentration of solution allowed the ductility of longitudinal direction to be greater than in the lateral direction. As a result, more metal was deposited in that area and formed a continuous metal coating. Thus, more defects were distributed in the lateral direction *versus* the longitudinal direction, affecting the conductivity as well. Secondly, when the concentration increased and the poplar was squeezed by test probes, the porous structure of wood allowed for the formation of craters in the lateral direction, which inhibited a continuous metal coating layer. Therefore, the resistivity in the lateral direction was higher than in the longitudinal direction.

Contact Angle and Surface Free Energy

As shown in Table 6, the poplar veneer contact angle was 35.1°, which is typical for a hydrophilic surface. Poplar is a porous material with a large number of hydroxyl groups on its surface, which means it is conducive to distilled water penetration. This contact angle would be expected to increase following copper plating. There are two main reasons for this phenomenon. First, the metal coating covered the pores such as rays, vessels, and pits on the poplar veneer surface, which effectively prevented water penetration. Secondly, based on the analysis previously, the metal coating surface exhibited a two levels structure, similar to a superhydrophobic lotus leaf structure. This hierarchical structure was not only able to enlarge the static contact angle from the surface water drops, but also produced small dynamic contact angle hysteresis, which led to hydrophobic characteristics. Additionally, it could reduce the possibility of deformation from water absorption by increasing the water repellency.

The veneer surface free energy decreased from 75.18 mJ/m² to 34.50 mJ/m². The surface free energy was the sum of the energy potential. Smaller values of surface free energy indicated more stable surface structure. Because distilled water has a high surface free energy and copper veneer has a low surface free energy, it is impossible that the energy flowed from low to high. According to this theory, the copper coating layer increased the hydrophobicity of the wood.

As the relative concentration increased, the polar component γ_i^p declined to zero. Because the metal coating covered the hydroxyl groups on the veneer surface, increasing the coating thickness resulted in a considerable decrease in γ_i^p . Therefore, the copper veneer surface free energy was completely dependent on γ_i^d .

Table 6. Surface Contact Angle and Free Energy

Plating Solution Dilution	Contact Angle (°) of Given Solvent		γ_i^d (mJ/m ²)	γ_i^p (mJ/m ²)	Surface Free Energy (γ_i)
	Water	Diiodomethane			
Negative	35.1	21.4	47.37	27.81	75.18
0.5	93.5	38.8	40.70	2.96	43.66
1.0	103.6	41.3	39.56	0	39.56
1.5	119.7	49.9	34.53	0	36.53
2.0	113.5	45.6	36.50	0	34.50

Table 6 shows that the relative concentration of 1.5 resulted in a greater contact angle than that of 2.0. The solid surface hydrophobic state was dependent on two factors: surface free energy and surface microstructure. When the intrinsic contact angle was greater than 90° , the surface roughness increased in accordance with the contact angle, which lead to a more hydrophobic solid surface. Based on the surface morphology analysis, the relative concentration of 1.5 resulted in the roughest copper veneer surface and the greatest contact angle.

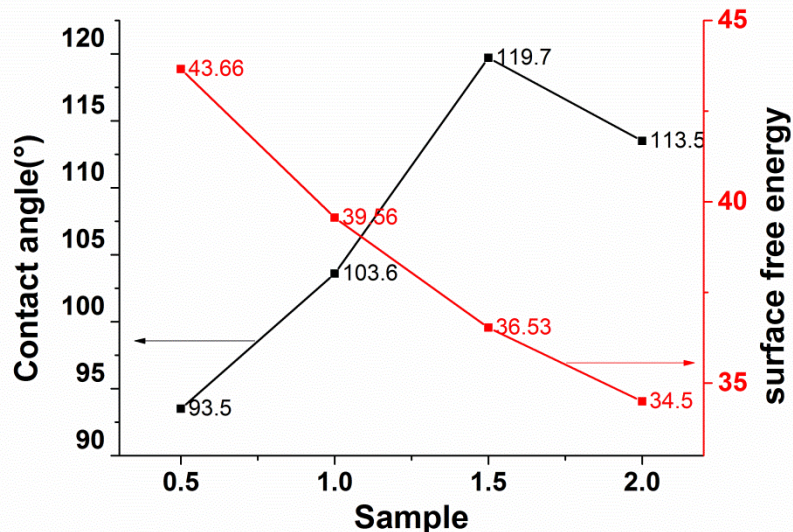


Fig. 5. The surface contact angle and surface free energy of electroless copper plated veneer at the concentration of 0.5, 1.0, 1.5, and 2.0

Electromagnetic Shielding Property

Figure 6a shows that the veneer had low electromagnetic shielding effectiveness at the relative concentration ratio of 0.5 (approximately 20 dB). The primary reason for this phenomenon was that the concentration was too low to form a complete and continuous metal coating on the surface. In addition, the electromagnetic waves could pass through the veneer from the exposed area, which seriously affected the electromagnetic shielding effectiveness. As shown in Table 7, the electromagnetic shielding effectiveness was greater than or equal to 50 dB. The values for the shielding effectiveness far exceeded the standard residential demand according to GJB2604-96 (1996) (> 45 dB).

Low-frequency electromagnetic wave shielding was better than high-frequency electromagnetic wave shielding, and the blue curve exhibited an upward trend (from 480 MHz to 1 GHz), which implied that the capability of electromagnetic shielding from high-frequency electromagnetic waves was improved. Thus, as the relative concentration increased, the copper coating on the surface of poplar veneer increased in integrity and density. Likewise, as the thickness of the coating increased, the ability of high-frequency electromagnetic wave shielding would be stronger.

Figure 6d corresponds to a relative concentration of 2.0, and it indicated that the maximum electromagnetic shielding effectiveness was 62 dB. Within the entire testing area, the electromagnetic shielding effectiveness ranged from 100k Hz to 1.5 GHz, and it was very stable.

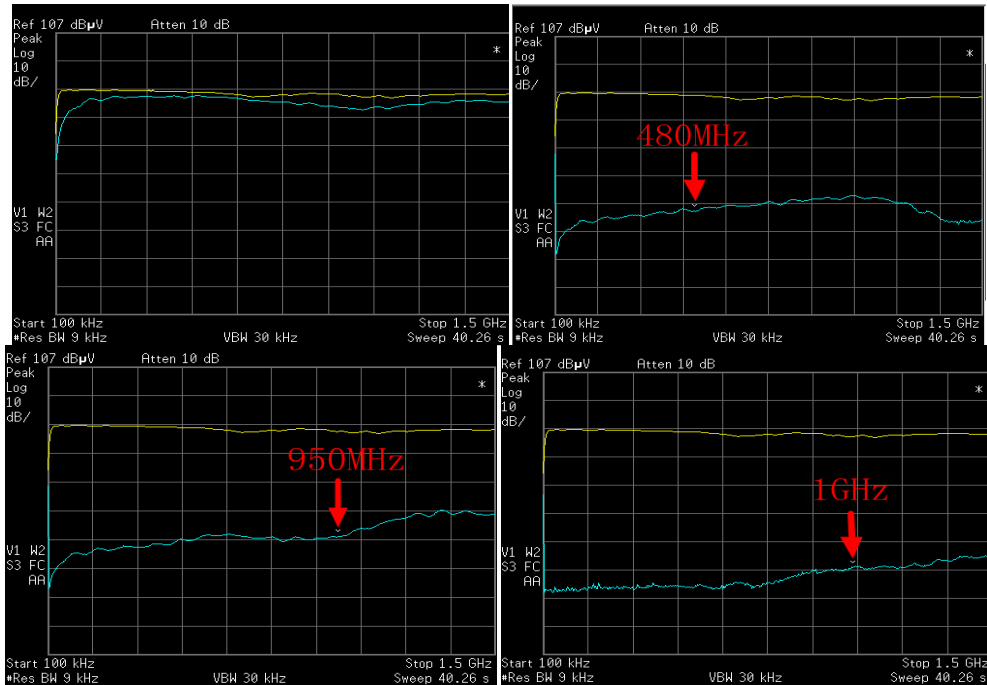


Fig. 6. Electromagnetic shielding curves at a relative concentration of A) 0.5; B) 1.0; C) 1.5; and D) 2.0

Table 7. Electromagnetic Shielding Effectiveness

Relative Concentration	Electromagnetic Shielding Effectiveness (dB)
0.5	20
1.0	50
1.5	55
2.0	62

CONCLUSIONS

1. The optimal solution concentration was 80 g/L of $\text{CuSO}_4 \cdot 5\text{H}_2\text{O}$, 20 g/L of $\text{C}_4\text{O}_6\text{H}_4\text{KNa}$, 40 g/L of EDTA-2Na, and 40 mL/L of HCHO.
2. The coating was face-centered and cubic in structure, and the grain size ranged from 17.4 nm to 30.7 nm.
3. The surface resistivity decreased as the coating thickness increased. The lateral direction measurement was approximately twice the measurement in the longitudinal direction.
4. The poplar veneer surface characteristics changed from hydrophilic to hydrophobic after copper plating. The surface free energy decreased as the concentration of the solution increased.
5. The optimal electromagnetic shielding effectiveness of the veneer was 62 dB.

ACKNOWLEDGMENTS

This work was supported by the Science and Technology Plan Projects (Grant No. 20130515), the Natural Science Foundation of Inner Mongolia Autonomous Region (Grant No. 2013MS0526), and the Science Research Innovation Projects of the Inner Mongolia Autonomous Region for Graduate (Grant No. B20151012911).

REFERENCES

- GJB2604 (1996). "Material shielding effectiveness test methods," COSTIND, Peking, China.
- Hanada, E., Takano, K., Antoku, Y., Matsumura, K., Watanabe, Y., and Nose, Y. (2002). "A practical procedure to prevent electromagnetic interference with electronic medical equipment," *Journal of Medical Systems* 26(1), 61-65. DOI: 10.1023/A:1013094904976
- Huang, J. T., and Zhao, G. J. (2004). "Electroless plating of wood," *Journal of Beijing Forestry University* 26(3), 88-92. DOI: 10.3321/j.issn:1000-1522.2004.03.018 (in Chinese)
- Huang, J. T., and Zhao, G. J. (2006). "Electroconductivity and electromagnetic-shielding effectiveness of nickel-plated veneer," *China Forest Products Industry* 33(1), 14-17. DOI: 10.3969/j.issn.1001-5299.2006.01.004 (in Chinese)
- Li, N. N., Li, G. L., Wang, H. D., and Kang, J. J. (2015). "Research progress of surface free energy's computing methods and the influence on the properties of material surface," *Materials Review* (11), 30-35. DOI: 10.11896/j.issn.1005-023X.2015.011.005 (in Chinese)
- Liu, Y. (2003). "The system of wooden environment evaluation," *Journal of Huazhong Agricultural* 22(5), 499-504. DOI: 10.3321/j.issn:1000-2421.2003.05.020 (in Chinese)
- Oka, H., and Hayakawa, H. (2002). "Laminated impregnated magnetic wood manufacturing methods and magnetic characteristics from DC to 135 GHz band," *IEEE Transactions on Magnetics* 38(5), 3327-3328. DOI: 10.1109/TMAG.2002.80311
- Oka, H., Hojo, A., Osada, H., Namizaki, Y., and Taniuchi, H. (2004). "Manufacturing methods and magnetic characteristics of magnetic wood," *Journal of Magnetism and Magnetic Materials* 272(Part 3), 2332-2334. DOI: 10.1016/j.jmmm.2003.12.1214
- Pi, J. H., and Wang, Z. Z. (2006). "The research status quo of wood-metal composite materials," *Journal of Nan Jing Institute of Technology (Natural Science Edition)* 4(2), 17-21. DOI: 10.3969/j.issn.1672-2558.2006.02.004 (in Chinese)
- Sittisart, P., Hyland, M., Hodgson, M., Nguyen, C., and Fernyhough, A. (2014). "Preparation and characterization of electroless nickel-coated cellulose fibres," *Wood Science & Technology* 48(4), 841-853. DOI: 10.1007/s00226-014-0643-2
- SJ20524 (1995). "Material shielding effectiveness test methods," Ministry of Industry and Information Technology, Peking, China.
- Wang, L. J., Li, J., and Liu, Y. X. (2004a). "Activation process of electroless plating poplar veneers," *Forestry Science & Technology* 29(3), 46-48. DOI: 10.3969/j.issn.1001-9499.2004.03.017 (in Chinese)

- Wang, L. J., Li, J., and Liu, Y. X. (2004b). "The effect of process conditions on properties of nickel-plate of the electroless nickel-plated poplar veneers," *Journal of Northeast Forestry University* 32(3), 37-39. DOI: 10.13759/j.cnki.dlxb.2004.03.011(in Chinese)
- Wang, L., Jian, L., and Liu, H. (2011). "A simple process for electroless plating nickel-phosphorus film on wood veneer," *Wood Science & Technology* 45(1) 161-167. DOI: 10.1007/s00226-010-0303-0
- Wang, L. J., Jian, L., and Liu, Y. X. (2006). "Preparation of electromagnetic shielding wood-metal composite by electroless nickel plating," *Journal of Forestry Research* 17(1), 53-56. DOI: 10.1007/s11676-006-0013-5
- Wang, L., and Li, J. (2013). "Electromagnetic-shielding wood-based material created using a novel electroless copper plating process," *BioResources* 8(3), 3414-3425. DOI: 10.15376/biores.8.3.3414-3425
- Zhang, X. Q., and Liu, Y. X. (2005). "Study on properties of steel/wood fiber composite MDF," *China Wood Industry* 19(2), 13-16. DOI: 10.3969/j.issn.1001-8654.2005.02.004 (in Chinese)
- Zhu, J. Q., Luo, C. H., and Huang, Z. N. (2001). "Composition of wire net and wood veneer," *China Wood Industry* 15(3), 5-7. DOI: 10.3969/j.issn.1001-8654.2001.03.002 (in Chinese)

Article submitted: March 31, 2016; Peer review completed: May 29, 2016; Revised version received: June 14, 2016; Accepted: June 16, 2016; Published: July 6, 2016. DOI: 10.15376/biores.11.3.6920-6931